Volcanic gas emissions and degassing dynamics at Ubinas and Sabancaya volcanoes; implications for the volatile budget of the...

Article *in* Journal of Volcanology and Geothermal Research · July 2017

DOI: 10.1016/j.jvolgeores.2017.06.027

CITATIONS
0

READS
24

14 authors, including:

C. Ian Schipper
French National Centre for Scientific Research
26 PUBLICATIONS **201** CITATIONS
SEE PROFILE

Masias Pablo
Instituto Geologico Minero Metalurgico, Peru
15 PUBLICATIONS **18** CITATIONS
SEE PROFILE

Philipson Bani
Institute of Research for Development
48 PUBLICATIONS **454** CITATIONS
SEE PROFILE

Manuel Moussallam
Deezer
14 PUBLICATIONS **50** CITATIONS
SEE PROFILE

Journal of Volcanology and Geothermal Research xxx (2017) xxx–xxx

Contents lists available at ScienceDirect

Journal of Volcanology and Geothermal Research

journal homepage: www.elsevier.com/locate/jvolgeores

Volcanic gas emissions and degassing dynamics at Ubinas and Sabancaya volcanoes; implications for the volatile budget of the central volcanic zone

Yves Moussallam [a,*], Giancarlo Tamburello [b,c], Nial Peters [a], Fredy Apaza [d], C. Ian Schipper [e], Aaron Curtis [f], Alessandro Aiuppa [b,g], Pablo Masias [d], Marie Boichu [h], Sophie Bauduin [i], Talfan Barnie [j], Philipson Bani [k], Gaetano Giudice [g], Manuel Moussallam [l]

[a] Department of Geography, University of Cambridge, Downing Place, Cambridge CB2 3EN, UK
[b] Dipartimento DiSTeM, Università di Palermo, Via archirafi 36, 90146 Palermo, Italy
[c] Istituto Nazionale di Geofisica e Vulcanologia, Sezione di Bologna, Via D. Creti 12, 40128 Bologna, Italy
[d] Observatorio Vulcanológico del Ingemmet (OVI), Arequipa, Peru
[e] School of Geography, Environment and Earth Sciences, Victoria University of Wellington, PO Box 600, Wellington 6140, New Zealand
[f] Department of Earth and Environmental Science, New Mexico Institute of Mining and Technology, 801 Leroy Place, Socorro, NM 87801, USA
[g] Istituto Nazionale di Geofisica e Vulcanologia, Sezione di Palermo Via La Malfa, 153, 90146 Palermo, Italy
[h] Laboratoire d'Optique Atmosphérique, Université Lille 1, CNRS/INSU, UMR8518, Villeneuve d'Ascq, France
[i] Spectroscopie de l'atmosphère, Service de Chimie Quantique et Photophysique, Université Libre de Bruxelles (ULB), Brussels, Belgium
[j] Department of Physical Sciences, The Open University, Walton Hall, Milton Keynes MK7 6AA, UK
[k] Laboratoire Magmas et Volcans, Univ. Blaise Pascale – CNRS – IRD, OPGC, 63000 Clermont-Ferrand, France
[l] Deezer, Research and Development, 10/12 rue d'Athènes, 75009 Paris, France

ARTICLE INFO

Article history:
Received 29 March 2017
Received in revised form 23 June 2017
Accepted 30 June 2017
Available online xxxx

Keywords:
Sabancaya
Ubinas
Carbon dioxide
Volcanic degassing
UV-camera
DOAS
Multi-GAS
IASI
Trail By Fire

ABSTRACT

Emission of volcanic gas is thought to be the dominant process by which volatiles transit from the deep earth to the atmosphere. Volcanic gas emissions, remain poorly constrained, and volcanoes of Peru are entirely absent from the current global dataset. In Peru, Sabancaya and Ubinas volcanoes are by far the largest sources of volcanic gas. Here, we report the first measurements of the compositions and fluxes of volcanic gases emitted from these volcanoes. The measurements were acquired in November 2015. We determined an average SO_2 flux of 15.3 ± 2.3 kg s^{-1} (1325-ton day^{-1}) at Sabancaya and of 11.4 ± 3.9 kg s^{-1} (988-ton day^{-1}) at Ubinas using scanning ultraviolet spectroscopy and dual UV camera systems. In-situ Multi-GAS analyses yield molar proportions of H_2O, CO_2, SO_2, H_2S and H_2 gases of 73, 15, 10 1.15 and 0.15 mol% at Sabancaya and of 96, 2.2, 1.2 and 0.05 mol% for H_2O, CO_2, SO_2 and H_2S at Ubinas. Together, these data imply cumulative fluxes for both volcanoes of 282, 30, 27, 1.2 and 0.01 kg s^{-1} of H_2O, CO_2, SO_2, H_2S and H_2 respectively. Sabancaya and Ubinas volcanoes together contribute about 60% of the total CO_2 emissions from the Central Volcanic zone, and dominate by far the total revised volatile budget of the entire Central Volcanic Zone of the Andes.

1. Introduction

Whilst volcanic SO_2 emissions can be measured from space at all strongly outgassing volcanoes (e.g., Carn et al., 2017), emissions of other gases still rely on ground-based measurements. Such measurements have only been performed on a fraction of all outgassing subaerial volcanoes (e.g., Burton et al., 2013). In order to determine the contribution of volcanic gases to the atmosphere and to quantify Earth's deep volatile cycle, a much larger number of measurements need to be performed. The total volcanic volatile flux is dominated by persistent degassing (Shinohara, 2013). Although impressive and punctually important, explosive eruptions typically contribute fifteen times less volatiles than persistent degassing does (Shinohara, 2008), such that total volatile flux is dominated by only a handful of persistently degassing volcanoes. Based on volcanoes with quantified emissions, ten volcanoes emit 67% of the estimated total volatile flux from subduction zones (Shinohara, 2013), while five volcanoes are thought to be responsible for 80% of the global CO_2 flux from subaerial volcanoes (Burton et al., 2013). Identifying and accurately measuring strongly emitting volcanoes is hence of paramount importance for an accurate global estimate to be achieved. High quality gas measurements however tend to be

* Corresponding author.
E-mail address: ym286@cam.ac.uk (Y. Moussallam).

http://dx.doi.org/10.1016/j.jvolgeores.2017.06.027

made preferentially on volcanoes in densely populated areas, and hence likely underestimate global flux (Shinohara, 2008).

The Central Volcanic Zone (CVZ) is part of the Andean Volcanic Belt and extends from Peru to Chile over a length of ~1500 km. This volcanic arc, related to a segment of the Nazca plate subduction zone, is home to 69 Holocene volcanoes (Global Volcanism Program, 2013), a significant proportion of which are persistently degassing. The region, however, has remained absent from global compilations of volcanic gas emissions (Andres and Kasgnoc, 1998; Burton et al., 2013; Fischer, 2008; Hilton et al., 2002; Pyle and Mather, 2009). The total volatile flux from Peruvian volcanoes in particular has never been measured.

Here we report compositional and flux data from two remote, persistently degassing volcanoes: Sabancaya and Ubinas (Fig. 1). Based on satellite detection of SO_2 (Carn et al., 2016, 2017), these two volcanoes are thought to account for the majority of the volcanic volatile flux from Peru and we find that they contribute two-thirds of the total estimated volatile flux from the CVZ.

2. Historical and current activity

2.1. Ubinas

Ubinas is Peru's most active volcano (Rivera et al., 1998; Thouret et al., 2005). Since its last Plinian eruption in ca. A.D. 1000–1160, the volcano had been in a nearly persistent state of unrest with twenty-three reported periods of increased activity (intense degassing, vulcanian, phreatomagmatic and phreatic eruptions) between 1550 and 1996 (Rivera et al., 1998, 2010; Thouret et al., 2005). Following eight months of heightened gas emissions, explosive activity (VEI 2) began at Ubinas in late March 2006. The activity increased between April and October 2006 then slowly decreased until December 2009 (Rivera et al., 2010, 2014). This episode of unrest, characterised by vulcanian explosions emitting juvenile material of andesitic composition, was the first crisis at Ubinas to be closely monitored by scientists (Rivera et al., 2010). In September 2013 eruptive activity resumed at Ubinas volcano (Coppola et al., 2015) and is ongoing at the time of writing. The current activity started with phreatic eruptions and is now characterised by vulcanian eruptions. On March 19, 2014, incandescent lava could be observed in the crater (Coppola et al., 2015). At the time of our investigation in November 2015 the eruption frequency was around one vulcanian eruption per week. In between eruptions a permanent and continuous translucent plume is observed.

2.2. Sabancaya

The first occidental written records of Sabancaya's activity can be found in 1750 and 1784–85 in the writings of the parish priest of Salamanca (Thouret et al., 1994). Activity in 1752 and 1784 are mentioned in Spanish chronicles (Travada and Córdova, 1752; Zacámola and Jáuregui, 1784) and may be associated with small regional ash deposits (Thouret et al., 1994). Low-level, intermittent fumarolic activity characterised the subsequent period, ending in 1986 when intense fumarolic activity resulted in a 500 to 1000 m high plume (Thouret et al., 1994). The activity increased gradually (Chorowicz et al., 1992)

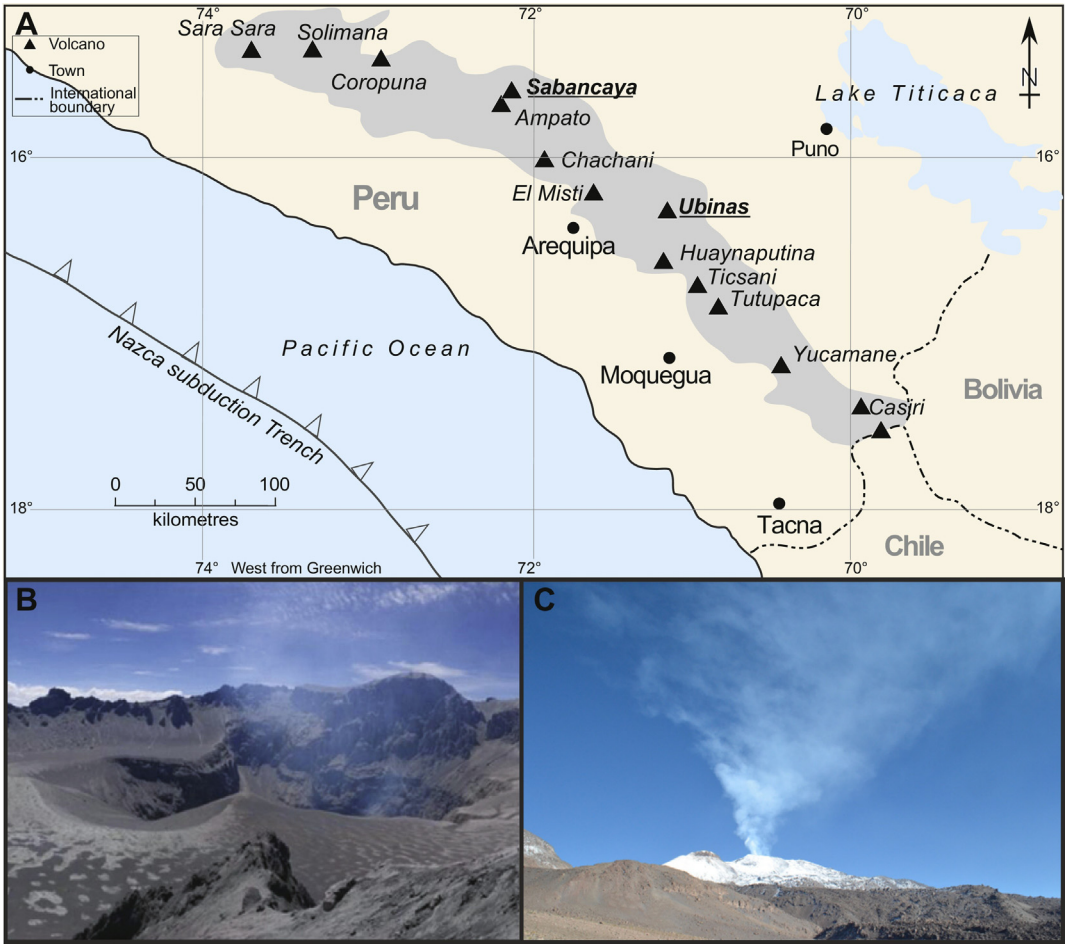

Fig. 1. A. Location map showing the location of Ubinas and Sabancaya volcanoes together with the location of all Peruvian Holocene volcanoes and the Nazca subduction trench. B. Photograph showing the clear plume vertically rising from Ubinas crater on November 23, 2015. Picture taken from the crater rim looking SSE. C. Photograph showing the clear plume vertically rising from Sabancaya crater on November 26, 2015. Picture taken from UV remote sensing location looking NNW.

Please cite this article as: Moussallam, Y., et al., Volcanic gas emissions and degassing dynamics at Ubinas and Sabancaya volcanoes; implications for the volatile budget of the centr..., J. Volcanol. Geotherm. Res. (2017), http://dx.doi.org/10.1016/j.jvolgeores.2017.06.027

eventually turning explosive on 28 May 1990. Explosive activity lasted eight years, being especially intense from 1990 to 1992 with plume heights at times reaching 7 km and ash falling as far as 12 km away from the volcano's summit (Gerbe and Thouret, 2004; Thouret et al., 1994). The juvenile material erupted during this period was andesitic and dacitic, spanning a narrow range of compositions (60–64 wt% SiO_2) and containing rare magmatic enclaves of andesitic composition (57 wt% SiO_2) (Gerbe and Thouret, 2004). Gerbe and Thouret (2004) proposed that the main magma body consisted of dacitic magmas which through repeated recharge of more mafic magmas led to the formation of hybrid andesites.

After 15 years of quiescence, fumarolic activity resumed at Sabancaya on 5 December 2012 and was followed by a strong increase in seismic activity starting in February 2013 (IGP 2013; OVI 2013; Jay et al., 2015). In August 2014 two phreatic eruptions were recorded and since June 2014 persistent degassing has been observed from the main crater (IGP 2014; OVI 2014). A persistent, continuous and translucent gas plume has been observed since November 2015, with plume heights varying from 250 to 1500 m above the vent since August 2014 (OVI 2015). On 6 November 2016, eleven months after our measurements, eruptions started producing ash plumes up the 3 km high and are ongoing at the time of writing.

3. Methods

3.1. Scanning DOAS

At Ubinas, horizontal scans transecting the plume just above the crater were made from a site 1.1 km away from the crater rim at S16.33360° W070.90854° at 5028 m a.s.l., with an inclination angle of 16° above horizontal. At Sabancaya volcano, horizontal scans were made from a site 4.1 km away from the crater rim at S15.824435° W071.843594°at 5036 m a.s.l., with an inclination angle of 12° above horizontal. In both cases the plume rose vertically before drifting horizontally with the wind (Fig. 1). Only scans that completely traversed the full plume-width were used to calculate emission rates. Data acquisition was paused whenever clouds formed within the field of view. A custom made scanner recorded angles with millisecond precision, and the scanning stage was in motion continuously, with spectra being recorded such that each spectrum is the average over 0.5 degrees of scan (see unit description in Moussallam et al., 2014, code available at: http://code.google.com/p/avoscan/). The spectrometer used was a Flame spectrometer manufactured by Ocean Optics (for specifications see: https://oceanoptics.com/product/flame-spectrometer/).

The acquisition of data and subsequent retrieval of SO_2 flux values followed the standard DOAS methodology (Platt and Stutz, 2008) using a fitting window of 316.5–330 nm. We used the solar spectrum measured by (Chance and Kurucz, 2010) and SO_2 and O_3 reference spectra measured by (Vandaele et al., 1994) and Burrows et al. (1999), respectively. Rise speeds for the plume and light dilution correction were estimated using UV camera images (see Section 3.2).

3.2. UV camera

Two dual UV Camera systems were deployed at Ubinas and Sabancaya volcanoes alongside a single scanning DOAS units. Both systems were equipped with passband filters centred at 310 nm, where SO_2 absorbs, and at 330 nm, outside the SO_2 absorption region. The first Apogee Alta U260 dual-set ultraviolet cameras (referred here as camera 1) were coupled to Pentax B2528-UV lenses, with focal length of 25 mm (FOV ~24°), and 10 nm full width at half maximum (FWHM) bandpass filters placed immediately in front of each lens (Asahi Spectra XBPA310 and XBPA330). The second JAI CM-140 GE-UV dual-set ultraviolet cameras (referred here as camera 2) are fitted with a 10 bit 1392 × 1040 pixels of Sony ICX407BLA UV-enhanced CCD array sensor. The JAI cameras (29 × 44 × 75 mm) are equipped with an electronic shutter architecture, a GiGE Vision interface and powered with a 12 V battery (~4 W). Two quartz lenses UKA optics UV1228CM (focal length 12 mm) provided an horizontal FOV ~41.7°, two passband filters (Edmund 310 nm CWL and 330 nm CWL nm, 10 nm full width high maximum) are placed between the lenses and the CCD array to avoid variations in wavelength response (Kern et al., 2013). Image acquisition and processing were achieved using Vulcamera, a stand-alone code specifically designed for measuring volcanic SO_2 fluxes using UV cameras (Tamburello et al., 2011). Every image acquired is saved in a 24 bit png pixmap with lossless compression. Two different sets of SO_2 calibration cells were used for the Apogee (94, 189, 475 and 982 ppm·m) and JAI (192, 1040 and 2003 ppm·m) UV camera systems to calibrate the qualitative measured apparent absorbance (Kantzas et al., 2010). Two parallel sections in our data series, perpendicular to the plume transport direction were used to derive plume speed (ranging from ~9 to 15 $m \cdot s^{-1}$). The data processing was carried out following the details outlined in Kantzas et al. (2010). A rough light dilution correction was achieved by assuming the average light intensity measured along the rocky flank of the volcanic edifice as a result of scattering of photons between the plume and the UV camera. The calculated average intensity values, for the 310 and 330 filtered images separately, were then subtracted from the raw images before calculating the apparent absorbance and SO_2 column density. Our calculated percentages of underestimation due to light dilution ranged from 29 to 38%, the same order of magnitude as those reported by Campion et al. (2015).

3.3. In situ gas measurements

Two portable Multi-GAS instruments (Shinohara, 2005) containing electrochemical and non-dispersive infrared (NDIR) sensors were deployed at Ubinas and Sabancaya volcanoes (at 16°20′22.73″S 70°54′ 0.87″W with an south-west going plume and at 15°47′20.63″S 71°51′ 20.83″W with a south-going plume respectively). The instruments were deployed at the NW side of the Ubinas crater (5570 m a.s.l) and southern side of the Sabancaya crater (5930 m a.s.l) on 23 November 2015 and 27 November 2015 respectively. The in-plume amount of volcanic gas species were measured at a 1 Hz frequency. CO_2 was measured by a NDIR sensor, H_2O was derived from relative humidity readings (Galltec sensors), providing a measuring range of 0–100% R.H. with an accuracy of ±2%.

The conversion from relative humidity to water mixing ratio was made following Buck (1981) and using the following equation:

$$H_2O = \frac{\left\{6.1121 \times \left(1.0007 + 3.46 \times P^{-6}\right) \times \exp\left[\frac{17.502 \times T}{240.97 + T}\right] \times \frac{Rh}{100} \times 10^6\right\}}{P} \quad (1)$$

where H_2O is the absolute water mixing ratio in ppmv, T is the temperature in °C, Rh is the relative humidity in % and P is the atmospheric pressure in mbar. The gas temperature used in this equation is measured in real time by the Multi-GAS, the pressure is also measured by the Multi-GAS and assumed to remain constant during the measurements. SO_2, H_2S and H_2 were measured via specific electrochemical sensors (respectively, models 3ST/F, EZ3H, and EZT3HYT "Easy Cal"; all from City Technology with calibration range of 0–200 ppm). The sensors, pump and data-logger are housed inside a weatherproof box and powered by a small (6 Ah) 12 V LiPo battery. Similar systems have now been successfully deployed at many volcanoes (e.g. Aiuppa et al., 2011, 2012, 2014, 2015; Moussallam et al., 2012, 2014, 2016, 2017) and the system used here is the same as Moussallam et al. (2016). All sensors were calibrated in the laboratory in late October 2015 with target gases of known amount. Post processing was performed using the Ratiocalc software (Tamburello, 2015). In the subsequent result section, H_2O and CO_2 mixing ratios are reported after subtraction of their mean

Please cite this article as: Moussallam, Y., et al., Volcanic gas emissions and degassing dynamics at Ubinas and Sabancaya volcanoes; implications for the volatile budget of the centr..., J. Volcanol. Geotherm. Res. (2017), http://dx.doi.org/10.1016/j.jvolgeores.2017.06.027

ambient air mixing ratios (measured by the Multi-GAS on the volcano flank directly prior to entering the plume), H_2S mixing ratios are reported after correction of laboratory-determined interference with SO_2 gas (typically 10–15%).

3.4. IASI observations

The Infrared Atmospheric Sounding Interferometer (IASI) is a Fourier transform spectrometer carried onboard the Met-Op A and B polar orbiting meteorological satellites which can provide global observations twice a day. IASI records infrared emission spectra from 645 to 2760 cm^{-1} at 0.25 cm^{-1} resolution (0.5 cm^{-1} after apodisation) with a pixel size of 12 km (at nadir) over a swath width of about 2200 km. Sabancaya and Ubinas volcanoes most often release SO_2 in the lower troposphere, which is difficult to detect by hyperspectral infrared IASI spaceborne instruments, whose sensitivity to this part of the atmosphere is limited by thermal contrast. However, recent studies have demonstrated the capability of IASI to measure near-surface SO_2 in the nu_3 band in case of high thermal contrast and low humidity (Bauduin et al., 2014, 2016). More particularly, Bauduin et al. (2016) have developed a specific algorithm, based on a look-up table approach, to retrieve near-surface SO_2 amounts from IASI measurements at a global scale. This algorithm is used in this work and provides monthly-mean 0–4 km SO_2 column amounts on a 0.25 × 0.25 horizontal grid for the months of October through December 2015 which surround the period of time when ground-based SO_2 measurements were performed. The retrieval strategy relies on the calculation of hyperspectral range indexes, which represent the strength of the nu_3 band (1300–1410 cm^{-1}) of SO_2 in IASI radiance spectra (Bauduin et al., 2016). Firstly, spectra with detectable SO_2 at low-altitude (below 4 km) are selected using the algorithm of Clarisse et al. (2014). Secondly, the conversion of indexes to SO_2 columns is carried out using look-up tables built from forward model simulations. Only SO_2 column amounts with relative error < 25% and absolute error < 10 DU are kept, which may create an overestimation of IASI averages, as discussed in Bauduin et al. (2016).

4. Results

4.1. SO_2 flux

Emission rates of SO_2 are shown in Fig. 2 as flux in kg s^{-1} and t d^{-1} for measurements made on the 22 and 23 November 2015 at Ubinas and 26 November 2015 at Sabancaya. We report only fluxes obtained during cloud-free periods where the plume was well defined and transparent, limiting the dataset to ~5 h of observations at Ubinas (~3 h on the 22nd starting at 10:13 local time and ~2 h on the 23rd starting at 08:27 local time) and ~1.5 h of observations at Sabancaya volcano starting at 10:09 local time. An average SO_2 emission rate of 12.0 ± 4.5 kg s^{-1} (equivalent to 1040 ± 390 t/day; error reported as one standard deviation) was measured by DOAS at Ubinas on the 23 November 2015 and an average SO_2 emission rate of 11.0 ± 5.9 kg s^{-1} (equivalent to 947 ± 508 t/day) was measured by UV camera at Ubinas on the 22 November 2015. Both measurements are very close and within error, indicating no resolvable day-to-day differences. The average SO_2

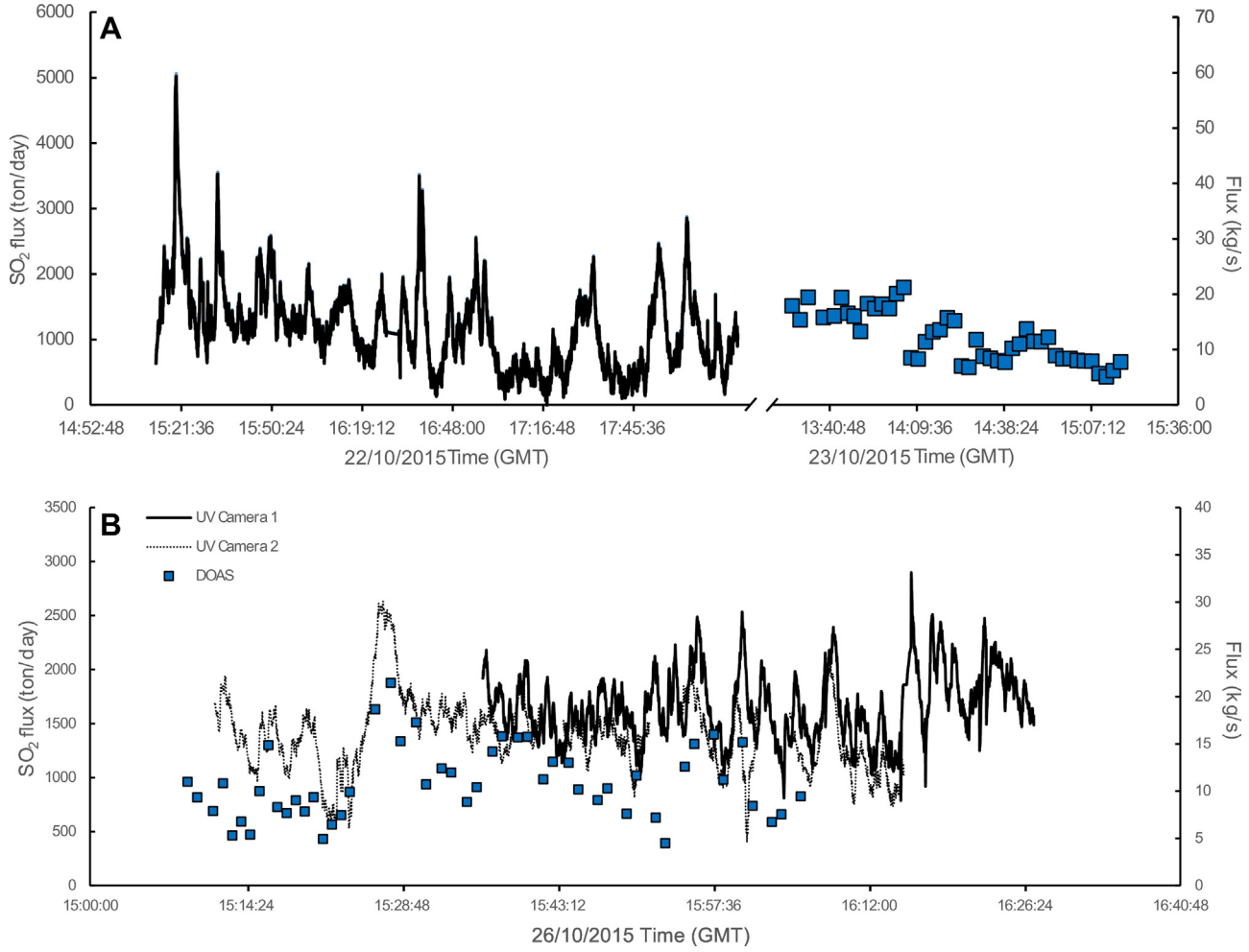

Fig. 2. SO_2 flux time series for (A) Ubinas volcano on 22 and 23 November 2015 as measured by UV camera 1 and scanning DOAS (B) Sabancaya volcano on 26 November 2015 as measured by UV camera 1, 2 and scanning DOAS. Average SO_2 fluxes are 1494 and 1663 ton/day with standard deviations of 919 and 318 ton/day for Ubinas and Sabancaya volcanoes respectively.

Please cite this article as: Moussallam, Y., et al., Volcanic gas emissions and degassing dynamics at Ubinas and Sabancaya volcanoes; implications for the volatile budget of the centr..., J. Volcanol. Geotherm. Res. (2017), http://dx.doi.org/10.1016/j.jvolgeores.2017.06.027

emission rate (average of both UV camera and DOAS data, weighted by acquisition time) at Ubinas volcano is 11.4 ± 3.9 kg s^{-1} (equivalent to 988 ± 333 t d^{-1}). On the 26 November 2015 at Sabancaya an average SO_2 emission rate of 19.2 ± 3.7 kg s^{-1} (equivalent to 1663 ± 318 t/day) was measured by UV camera 1, an average SO_2 emission rate of 16.1 ± 4.1 kg s^{-1} (equivalent to 1394 ± 352 t/day) was measured by UV camera 2 and an average SO_2 emission rate of 11.0 ± 3.8 kg s^{-1} (equivalent to 947 ± 332 t/day) was measured by DOAS. Both UV cameras show extremely similar results while the DOAS scans systematically yield slightly lower fluxes (Fig. 2). Given that each technique is different and suffers limitations (e.g., more accurate retrieval procedure for DOAS compared to UV cameras, higher frequency observations for UV Camera compared to the DOAS scans) differences are not surprising but importantly all averaged SO_2 fluxes during the observation period are within error (all reported errors are one standard deviation). The average SO_2 emission rate (average of both UV cameras and DOAS data, weighted by acquisition time) at Sabancaya volcano is 15.5 ± 2.3 kg s^{-1} (equivalent to 1325 ± 196 t d^{-1}). Fig. 2 shows very large variations in the SO_2 emissions at Ubinas volcano over timescale of tens of minutes to hours, tracking the "puffing" outgassing activity. Variations are also apparent in the SO_2 emissions at Sabancaya volcano and are of lower amplitude and higher frequency than at Ubinas.

4.2. Gas composition

At Ubinas, two Multi-GAS units ran for about 2.5 h during ascent of the volcano as to sample episodic patches of wind-blown plume. During the measurement period the Ubinas plume was found to be very dilute (max 8 ppm SO_2). In addition, the measurements indicate that several sources were contributing to the gas signal (i.e. low temperature fumaroles participated in the recorded signal, mainly contaminating the CO_2 and H_2O signal). In order to isolate the magmatic plume end-member we only considered measurement periods during which the densest part of the plume was sampled (Fig. 3). In order to obtain the volcanic CO_2/SO_2 ratio we plotted the apparent CO_2/SO_2 ratio measured as a function of SO_2 amount measured at the same time, using SO_2 as the indicator of volcanic gas. Fig. 3(C) shows that while the recorded CO_2/SO_2 ratio ranges considerably (from 1 to >30) at the low SO_2 range (<3 ppm), it converges at a single value of ~1.8 in the densest plume (high SO_2). The resulting ratios are listed in Table 1. Due to the very dilute nature of the plume, these data are associated with a larger error than typical Multi-GAS measurements.

At Sabancaya, we obtained 45 min of very good quality measurements (very high volcanic gas signal) with two Multi-GAS instruments sampling the plume at the crater rim. Fig. 4 shows four scatter plots of SO_2 vs CO_2; H_2O; H_2S and H_2 mixing ratios in the Sabancaya plume. The strong positive co-variations observed between SO_2 and the other detected volatiles confirm a single, common, volcanic origin. The gas/SO_2 molar plume ratios were obtained by calculating the gradients of the best-fit regression lines. The resulting ratios and associated errors are listed in Table 1.

During the acquisition period at the summit of Sabancaya, multiple explosions were heard deep inside the crater. Looking at the time series of Multi-GAS measurements, specific periods can clearly be highlighted as compositionally different. Fig. 5(A) and (B) highlights two such periods (referred to as pulse 1 and pulse 2) on the CO_2 vs SO_2 scatter plot obtained by the two Multi-GAS instruments. Fig. 5(C), (D), (E) and (F) show a time series, for a similar period on both instruments, during which a change in CO_2/SO_2 ratio occurs. These changes are not necessarily correlated with SO_2 mixing ratio (i.e. are not a data processing artefact) and cannot be attributed to instrumental noise as they are clearly recorded by both Multi-GAS instruments (Fig. 5(G)).

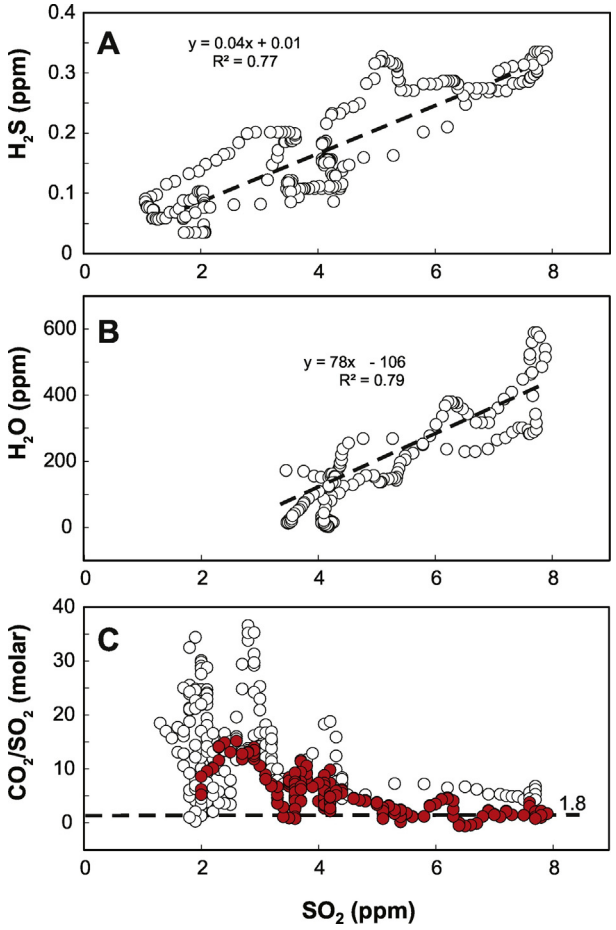

Fig. 3. (A) H_2S and (B) H_2O vs SO_2 scatter plots of the mixing ratios in the Ubinas plume. Only measurements taken in the densest part of the plume are considered (>1 ppmv SO_2 for the H_2S vs SO_2 scatter plot and >3.5 ppmv SO_2 for the H_2O vs SO_2 scatter plot). This corresponds to eight minutes of measurements presented in the H_2S vs SO_2 scatter plot and five minutes of measurements presented in the H_2O vs SO_2 scatter plot. Least-square regression lines are shown as black dotted lines on each plot. (C) CO_2/SO_2 ratio against SO_2 mixing ratio. In the densest part of the plume (SO_2 > 5 ppmv) the CO_2/SO_2 ratio converges to 1.8. The largest peaks recorded during the measurement (time periods where the CO_2 and SO_2 sensors recorded a clear response) period are shown as red dots. All measurements were taken on November 23, 2015 at an acquisition frequency of 2 Hz. (For interpretation of the references to colour in this figure legend, the reader is referred to the web version of this article.)

5. Discussion

5.1. Gas emissions from Peru and the CVZ

Ubinas and Sabancaya volcanoes are two strong sources of volatile flux to the atmosphere. Together they contribute nearly 1 Mt./yr (~2500 t/d) of CO_2 and SO_2, placing them in the top 15 volcanic emitters on the planet (Burton et al., 2013; Carn et al., 2017; Shinohara, 2013). At the time of writing they are the only two Peruvian volcanoes emitting appreciable amount of gases (i.e. amount high enough to be detected by ground-based spectroscopic techniques). The volatile fluxes presented in Table 1 therefore account for the bulk volatile emissions in the country of Peru. At the scale of the Central Volcanic Zone (CVZ), Ubinas and Sabancaya are found to be largest identified emitters of CO_2 and SO_2 (see previous compilation by Tamburello et al., 2014). These two volcanoes bring the total measured CO_2 flux of the CVZ from 1506 t/d to 4093 t/d, the total measured SO_2 flux from 1818 t/d to 4131 t/d and the total measured volatile flux from 20,220 to 49,587 t/d. Our ground-based measurements hence indicate that about 60% of the total volatile flux of the CVZ is produced by Ubinas and Sabancaya volcanoes. To put our ground-based measurements into context it is

Please cite this article as: Moussallam, Y., et al., Volcanic gas emissions and degassing dynamics at Ubinas and Sabancaya volcanoes; implications for the volatile budget of the centr..., J. Volcanol. Geotherm. Res. (2017), http://dx.doi.org/10.1016/j.jvolgeores.2017.06.027

Table 1
X/SO_2 molar and mass ratios measured by Multi-GAS and gas composition of the plume at Ubinas and Sabancaya volcanoes. The inferred flux range of each species is based on an SO_2 flux estimate for each volcano. Error are expressed as the standard error of the regression analysis and subsequent error propagation, error on inferred flux propagate error on the SO_2 fluxes and gas ratios.

Volcano	Gas	Molar ratio (X/SO_2)	Error (1σ)	Mass ratio (X/SO_2)	Error (1σ)	Composition (mol%)	Error (1σ)	Flux (ton/day)	Error (1σ)	Flux (kg/s)	Error (1σ)
Ubinas	H_2O	**78**	30	**21.93**	8.44	**96.49**	37.11	**21,667**	11,084	**250.8**	128.3
	CO_2	**1.80**	0.50	**1.24**	0.34	**2.23**	0.62	**1222**	534	**14.1**	6.2
	SO_2	**1.00**	0.00	**1.00**	1.00	**1.24**	0.00	**988**	333	**11.4**	3.9
	H_2S	**0.04**	0.01	**0.02**	0.0053	**0.05**	0.012	**21**	9	**0.24**	0.10
Sabancaya	H_2O	**7.24**	0.33	**2.04**	0.09	**73.37**	3.34	**2698**	417	**31.2**	4.8
	CO_2	**1.50**	0.13	**1.03**	0.09	**15.20**	1.32	**1366**	234	**15.8**	2.7
	SO_2	**1.00**	0.00	**1.00**	1.00	**10.13**	0.00	**1325**	196	**15.3**	2.3
	H_2S	**0.11**	0.01	**0.06**	0.0053	**1.15**	0.101	**80**	14	**0.9**	0.2
	H_2	**0.015**	0.001	**0.0005**	0.00003	**0.152**	0.010	**0.6**	0.1	**0.007**	0.001

interesting to compare them with IASI observations over the period 2012 to 2015 (Fig. 6; Animation). Fig. 6 shows monthly mean 0–4 km SO_2 column amounts retrieved from IASI measurements over the CVZ for the month of February 2012 to 2015, April 2012 to 2015 and average over the months of October to December 2012 to 2015 while the animation shows monthly mean for every month from January 2012 to December 2015. Outgassing activity at Sabancaya can be seen to begin in late 2012 and at Ubinas in late 2013. Prior to this, outgassing in the CVZ was restricted to volcanic activity in northern Chile, with Lascar, Lastaria, Ollague, Irruputuncu, Isluga and Guallatirri likely to be the main sources (Animation). Since 2014 tropospheric SO_2 outgassing over the CVZ is clearly dominated by emissions from Sabancaya and Ubinas.

5.2. Degassing behaviour at Sabancaya

The time series recorded by the two Multi-GAS instruments at Sabancaya (Fig. 5(G)) shows clear fluctuations in the composition of gases emitted. An autocorrelation analysis (using averaged values from both instruments in order to reduce instrumental noise) reveals a clear periodicity in the gas compositional signal at ~4 min (Fig.

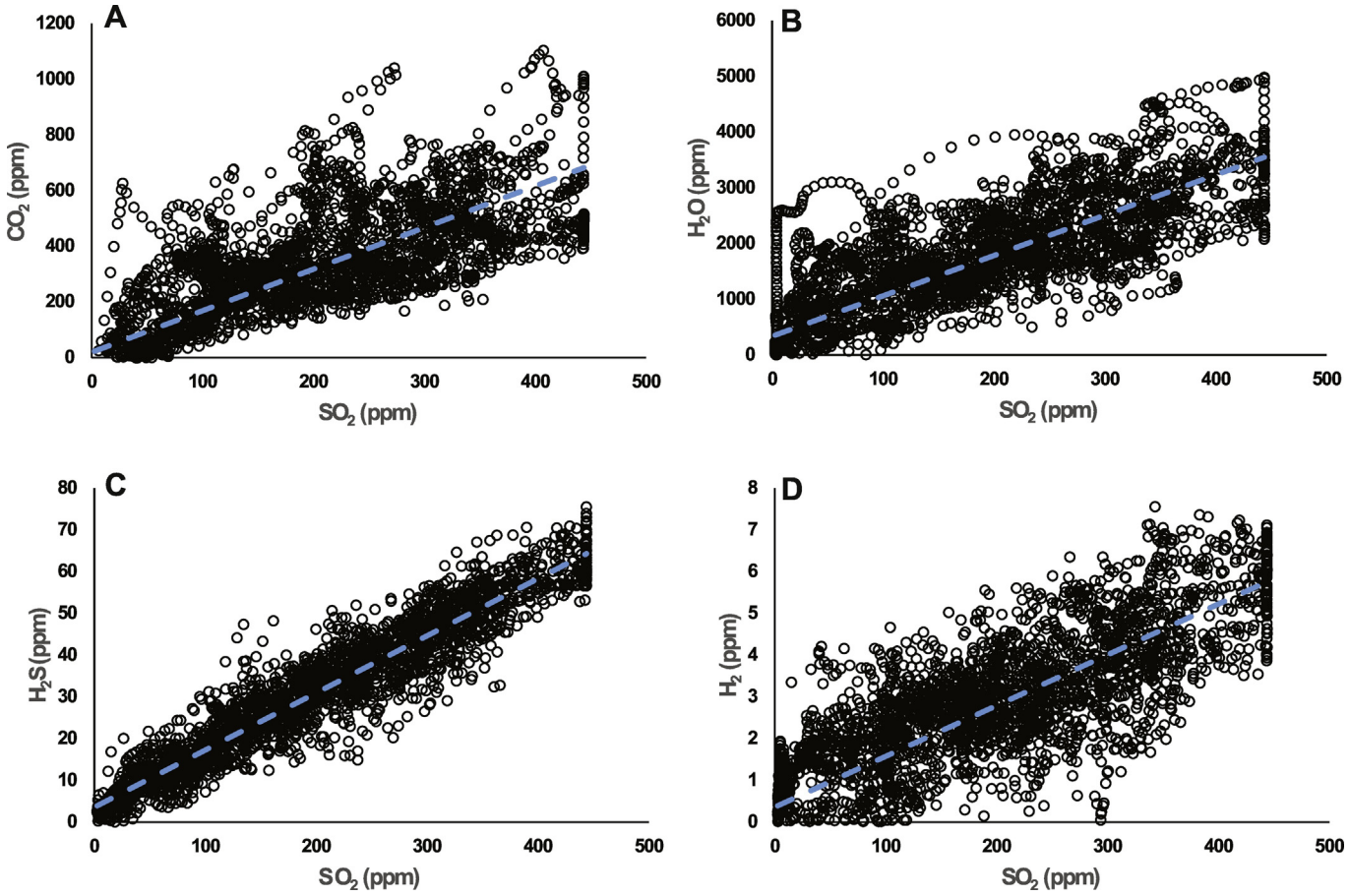

Fig. 4. (A) CO_2, (B) H_2O, (C) H_2S and (D) H_2 vs SO_2 scatter plots of the mixing ratios in the Sabancaya plume. Measurements were taken on November 27, 2015 for 45 min at an acquisition frequency of 1 Hz. Least-square regression lines are shown in dotted blue on each plot. (For interpretation of the references to colour in this figure legend, the reader is referred to the web version of this article.)

Please cite this article as: Moussallam, Y., et al., Volcanic gas emissions and degassing dynamics at Ubinas and Sabancaya volcanoes; implications for the volatile budget of the centr..., J. Volcanol. Geotherm. Res. (2017), http://dx.doi.org/10.1016/j.jvolgeores.2017.06.027

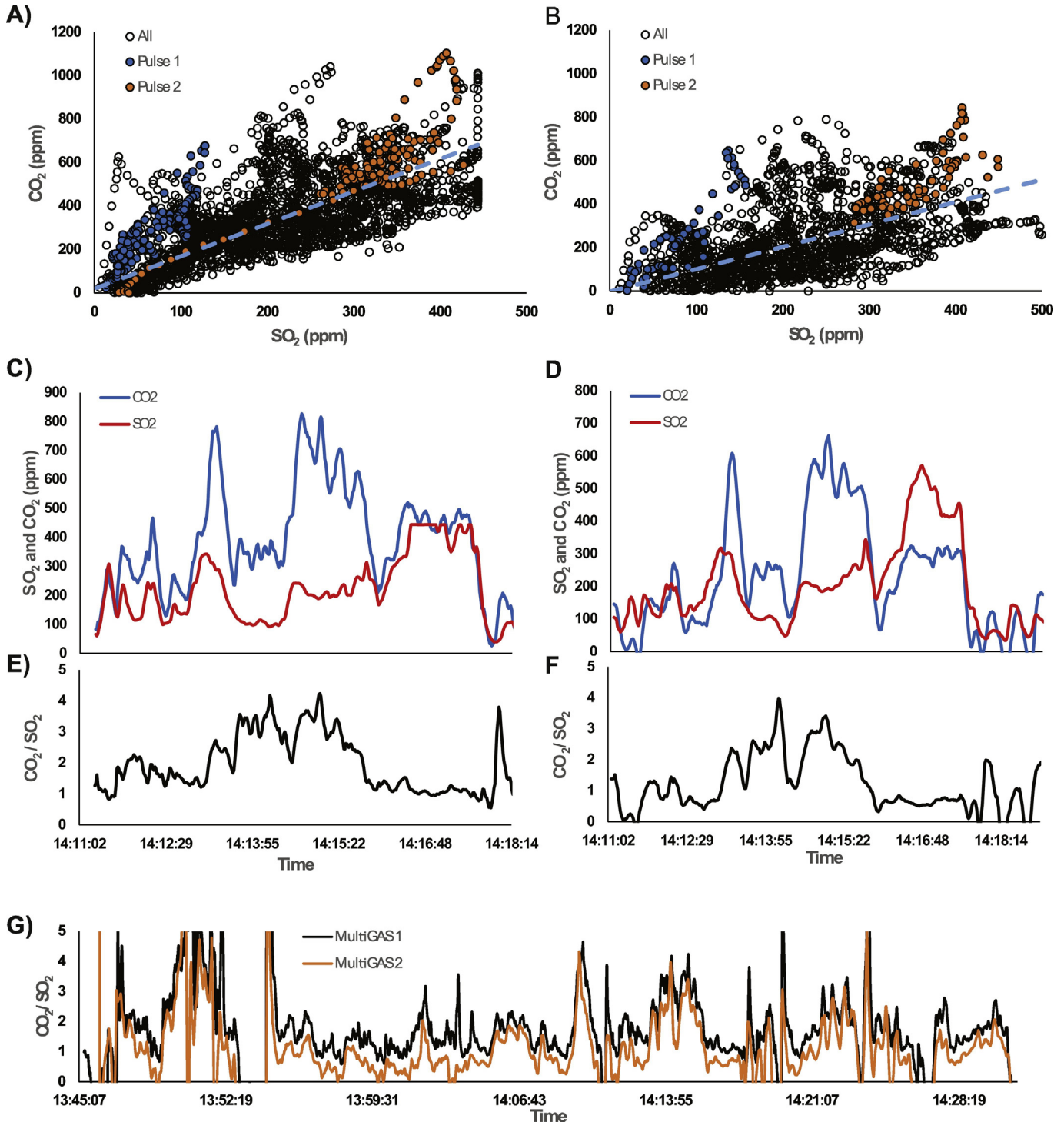

Fig. 5. CO_2 vs SO_2 scatter plots for Multi-GAS 1 (A) and 2 (B) on Sabancaya, showing the mixing ratio recorded during two "pulses". Time series of CO_2, SO_2 and CO_2/SO_2 ratio during a "pulse" as recorded by the first (C), (E) and second (D), (F) Multi-GAS instruments. (G) Complete time series of CO_2/SO_2 ratio as recorded by both Multi-GAS instruments and showing clear oscillations in the gas composition.

7(A)). The normalised autocorrelation formula is expressed as:

$$a(l) = \frac{\sum x(n) \times x(n-l)}{\sum x(n)^2} \quad (2)$$

where $x(n)$ is the centred time series and l the lag. Time series analyses of the SO_2 flux (Fig. 2) also show clear fluctuations for which autocorrelation analysis reveals two clear periodicities at ~2 and ~7 min (Fig. 7(B)). Whilst operating at a similar timescale, the periodicities recorded by both datasets do not match exactly. Possible reasons for this discrepancy are (i) atmospheric processes disturbing the gas flux prior to its measurement by the UV camera (ii) differing observation periods between both datasets and (iii) true absence of correlation between the two datasets. From our observations, none of these processes can be entirely ruled out.

Periodicities in the gas compositional and flux signals have been extensively documented at Erebus volcano (e.g. Oppenheimer et al., 2009; Boichu et al., 2010; Moussallam et al., 2012; Peters et al., 2014) and

Please cite this article as: Moussallam, Y., et al., Volcanic gas emissions and degassing dynamics at Ubinas and Sabancaya volcanoes; implications for the volatile budget of the centr..., J. Volcanol. Geotherm. Res. (2017), http://dx.doi.org/10.1016/j.jvolgeores.2017.06.027

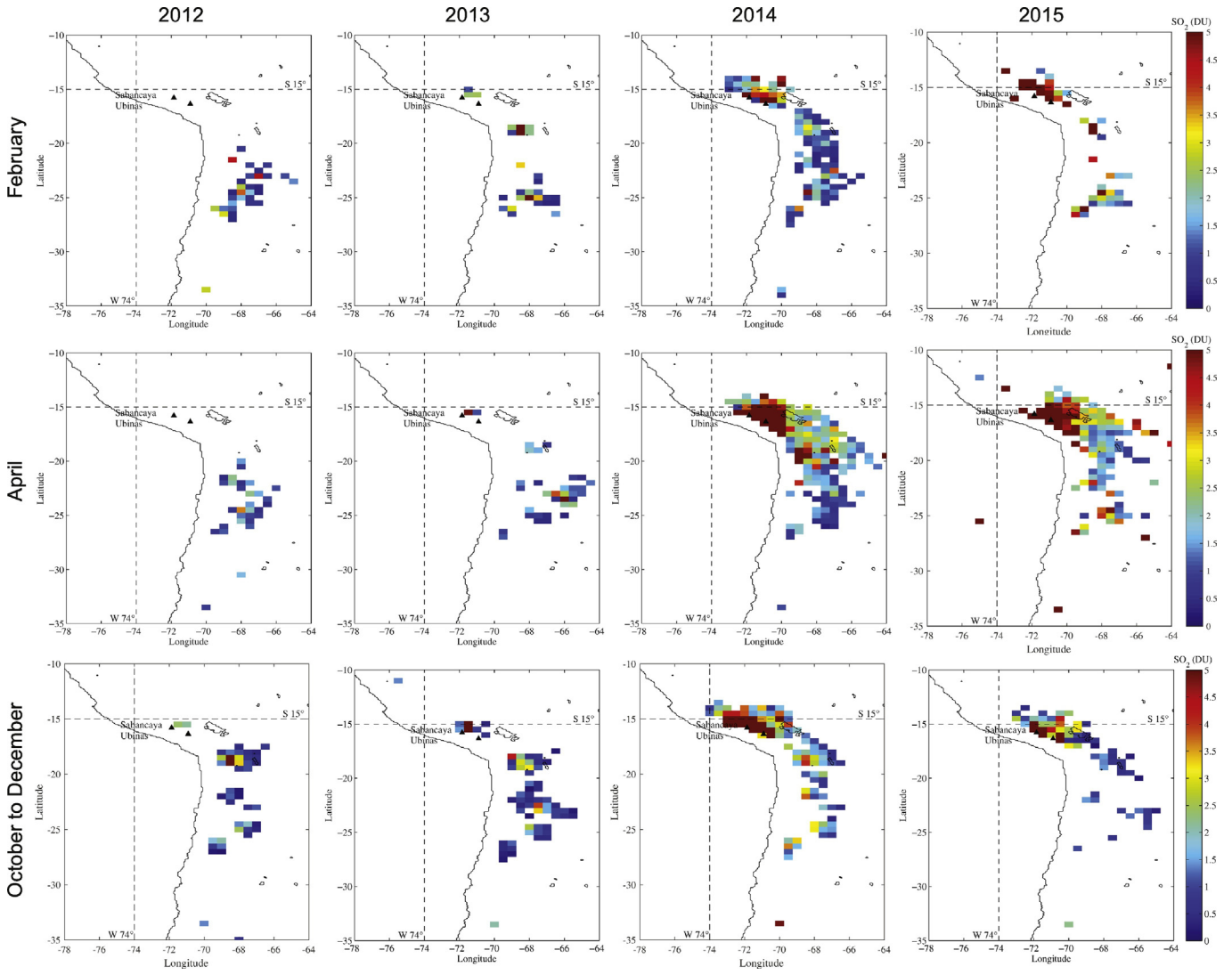

Fig. 6. Monthly mean 0–4 km SO_2 column amounts retrieved from IASI measurements in Peru and northern Chile for the months of February 2012 to 2015, April 2012 to 2015 and average over the months of October to December 2012 to 2015.

identified at Etna (Pering et al., 2014; Tamburello et al., 2013) and Ambrym volcanoes (Allard et al., 2016). This is the first time however, that such periodic gas signals are measured at a passively degassing dacitic volcano. Periodic degassing behaviour at passively degassing volcanoes has been attributed to magma convection in the volcanic conduit (e.g. Oppenheimer et al., 2009; Moussallam et al., 2015) or to the periodic release of over-pressurised gas slugs (e.g. Tamburello et al., 2013). At Sabancaya we found no correlation between the observed gas signal oscillations and seismic activity, suggesting that a seismically "quiet" process is responsible for the gas signal (the seismic network in November 2015 consisted of nine stations, the closest 1.6 km away from the summit). We therefore favour conduit convection and the cyclic input of deeper, gas-rich magma to shallow depth as the process responsible for the observed gas signal fluctuations at Sabancaya. This process can also readily explain the strong persistent degassing observed at the volcano since June 2014 with – at the time of our field measurements (November 2015) – no confirmed expulsion of juvenile magma. Our observations support studies performed at Japanese volcanoes (Kazahaya et al., 1994; Shinohara and Tanaka, 2012) in suggesting that magma convection in volcanic conduits is a common process happening over a large range of melt compositions.

5.3. Magmatic conditions at Sabancaya

Using the measured H_2O/H_2 and SO_2/H_2S ratios, the gas-melt equilibrium temperature and oxygen fugacity at Sabancaya can be calculated based on the reactions:

$$H_2 + ½O_2 = H_2O \quad (3)$$

and

$$H_2S + 3/2O_2 = SO_2 + H_2O \quad (4)$$

The direction and extent to which these reactions will proceed is a function of temperature and oxygen fugacity. Following Giggenbach (1987, 1996) and using the thermodynamic data of Stull et al. (1969) we can write the following equations:

$$\log\frac{H_2}{H_2O} = -\frac{12707}{T} + 2.548 - \frac{1}{2}\log fO_2 \quad (5)$$

Please cite this article as: Moussallam, Y., et al., Volcanic gas emissions and degassing dynamics at Ubinas and Sabancaya volcanoes; implications for the volatile budget of the centr..., J. Volcanol. Geotherm. Res. (2017), http://dx.doi.org/10.1016/j.jvolgeores.2017.06.027

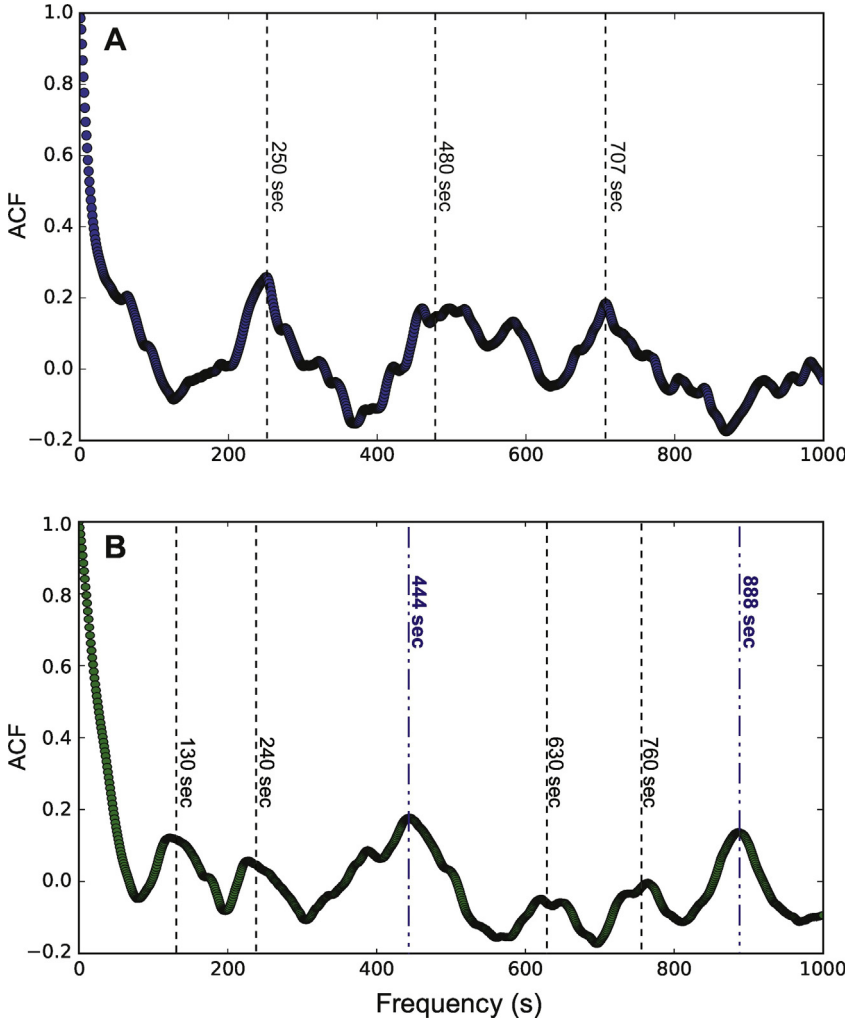

Fig. 7. Autocorrelation plots for (A) CO_2/SO_2 ratio as measured by the two Multi-GAS instruments on Sabancaya (using averaged values) during a 50 min acquisition period (B) SO_2 flux as measured by UV camera for a 51 min acquisition period. In (A) a clear periodicity occurs at ~4 min, as shown by three peaks in the autocorrelation (the peaks at 480 and 707 s are near multiples of the first peak). In (B) two periodicities can be resolved, one at ~2 min showing multiple harmonics and a second one at ~7 min shown by the two peaks at 444 and 888 s.

and

$$\log\frac{SO_2}{H_2S} = \frac{27377}{T} - 3.986 + \frac{3}{2}\log fO_2 - \log fH_2O \quad (6)$$

Given that the H_2/H_2O ratio, SO_2/H_2S ratio and the fugacity of H_2O are known (at atmospheric pressure, the fugacity of a gas is equal to its partial pressure), the equilibrium temperature and oxygen fugacity can be calculated (two equations with two unknown). This yields an equilibrium temperature of 730 °C and a logfO_2 equivalent to ΔQFM = +1.4 (where QFM refers to the quartz-fayalite-magnetite buffer, and where ΔQFM = logfO_2 − logfO_2 of QFM at corresponding temperature) or ΔNNO = +0.6 (where NNO refers to the Nickel Nickel-Oxide buffer, and where ΔNNO = logfO_2 − logfO_2 of NNO at corresponding temperature).

The main magma body involved in the 1990–1998 eruption of Sabancaya consisted of dacitic magmas periodically recharged by more mafic magmas leading to the formation and subsequent eruption of hybrid Andesite (Gerbe and Thouret, 2004). The gas-melt equilibrium conditions we calculate using the gas composition are entirely consistent (in terms of temperature) with equilibrium with a dacitic magma, but can only be considered a minimum estimate of the magmatic temperature. Continued measurements of the gas composition at Sabancaya could be extremely valuable for eruption forecasting. An increased frequency or magnitude of mafic input in the magmatic reservoir for instance, should lead to an increase in computed gas-melt equilibrium temperature.

6. Conclusion

We measured the composition and flux of gases emitted from Ubinas and Sabancaya volcanoes in November 2015 using scanning ultraviolet spectrometers, UV cameras, Multi-GAS instruments and IASI observations. Given that these volcanoes are the only significant sources of volcanic emissions to the atmosphere in Peru, we estimate the total CO_2 flux of Peruvian volcanoes to 2587 ± 767 t/d, the total SO_2 flux to 2313 ± 529 t/d and the total volatile flux at 29367 ± 12,819 t/d. Considering these two volcanoes more than doubles previous estimates of CO_2 and total volatile fluxes for the entire CVZ. At the global scale, these volcanoes rank in the top 15 emitters of CO_2 and SO_2. The gas compositions measured at both volcanoes has a clear magmatic signature implying that magma is efficiently being circulated at shallow depth and degassed within the volcanic conduit. Periodic oscillations in the gas composition at Sabancaya volcano further attest to probable vigorous convection of magma within the shallow conduit of this volcano.

Supplementary data to this article can be found online at http://dx.doi.org/10.1016/j.jvolgeores.2017.06.027.

Please cite this article as: Moussallam, Y., et al., Volcanic gas emissions and degassing dynamics at Ubinas and Sabancaya volcanoes; implications for the volatile budget of the centr..., J. Volcanol. Geotherm. Res. (2017), http://dx.doi.org/10.1016/j.jvolgeores.2017.06.027

Acknowledgements

This research was conducted as part of the "Trail By Fire" expedition (PI: Y. Moussallam). The project was supported by the Royal Geographical Society (with the Institute of British Geographers) with the Land Rover Bursary; the Deep Carbon Observatory DECADE Initiative; Ocean Optics; Crowcon; Air Liquide; Thermo Fisher Scientific; Cactus Outdoor; Turbo Ace and Team Black Sheep. We thank Jean-loup Guyot, Sebastien Carretier, Rose-Marie Ojeda, Pablo Samaniego and Jean-Luc Lepennec together with IRD South-America personnel for all their logistical help. We are extremely grateful to Marco Rivera and all OVI personnel for their help and support. YM acknowledges support from the Scripps Institution of Oceanography Postdoctoral Fellowship program. A.A and G.T acknowledge the ERC grant n. 305377 (BRIDGE). CIS acknowledges a research startup grant from Victoria University of Wellington. MB acknowledges support from the VOLCPLUME ANR-funded project.

References

Aiuppa, A., Shinohara, H., Tamburello, G., Giudice, G., Liuzzo, M., Moretti, R., 2011. Hydrogen in the gas plume of an open-vent volcano, Mount Etna, Italy. J. Geophys. Res. 116. http://dx.doi.org/10.1029/2011JB008461 (2011 8 PP).

Aiuppa, A., Giudice, G., Liuzzo, M., Tamburello, G., Allard, P., Calabrese, S., Chaplygin, I., McGonigle, A.J.S., Taran, Y., 2012. First volatile inventory for Gorely volcano, Kamchatka. Geophys. Res. Lett. 39, L06307. http://dx.doi.org/10.1029/2012GL051177.

Aiuppa, A., Robidoux, P., Tamburello, G., Conde, V., Galle, B., Avard, G., Bagnato, E., De Moor, J.M., Martínez, M., Muñóz, A., 2014. Gas measurements from the Costa Rica–Nicaragua volcanic segment suggest possible along-arc variations in volcanic gas chemistry. Earth Planet. Sci. Lett. 407:134–147. http://dx.doi.org/10.1016/j.epsl.2014.09.041.

Aiuppa, A., Bani, P., Moussallam, Y., Di Napoli, R., Allard, P., Gunawan, H., Hendrasto, M., Tamburello, G., 2015. First determination of magma-derived gas emissions from Bromo volcano, eastern Java (Indonesia). J. Volcanol. Geotherm. Res. 304:206–213. http://dx.doi.org/10.1016/j.jvolgeores.2015.09.008.

Allard, P., Burton, M., Sawyer, G., Bani, P., 2016. Degassing dynamics of basaltic lava lake at a top-ranking volatile emitter: Ambrym volcano, Vanuatu arc. Earth Planet. Sci. Lett. 448:69–80. http://dx.doi.org/10.1016/j.epsl.2016.05.014.

Andres, R.J., Kasgnoc, A.D., 1998. A time-averaged inventory of subaerial volcanic sulfur emissions. J. Geophys. Res. Atmos. 103:25251–25261. http://dx.doi.org/10.1029/98JD02091.

Bauduin, S., Clarisse, L., Clerbaux, C., Hurtmans, D., Coheur, P.-F., 2014. IASI observations of sulfur dioxide (SO_2) in the boundary layer of Norilsk. J. Geophys. Res. Atmos. 119:4253–4263. http://dx.doi.org/10.1002/2013JD021405.

Bauduin, S., Clarisse, L., Hadji-Lazaro, J., Theys, N., Clerbaux, C., Coheur, P.-F., 2016. Retrieval of near-surface sulfur dioxide (SO_2) concentrations at a global scale using IASI satellite observations. Atmos. Meas. Tech. 9:721–740. http://dx.doi.org/10.5194/amt-9-721-2016.

Boichu, M., Oppenheimer, C., Tsanev, V., Kyle, P., 2010. High temporal resolution SO_2 flux measurements at Erebus volcano, Antarctica. J. Volcanol. Geotherm. Res. 190:325–336. http://dx.doi.org/10.1016/j.jvolgeores.2009.11.020.

Burrows, J.P., Richter, A., Dehn, A., Deters, B., Himmelmann, S., Voigt, S., Orphal, J., 1999. Atmospheric remote-sensing reference data from GOME-2. Temperature-dependent absorbtion cross sections of O3 in the 231–794 nm range. J. Quant. Spectrosc. Radiat. Transf. 61:509–517. http://dx.doi.org/10.1016/S0022-4073(98)00037-5.

Burton, M.R., Sawyer, G.M., Granieri, D., 2013. Deep carbon emissions from volcanoes. Rev. Mineral. Geochem. 75:323–354. http://dx.doi.org/10.2138/rmg.2013.75.11.

Campion, R., Delgado-Granados, H., Mori, T., 2015. Image-based correction of the light dilution effect for SO_2 camera measurements. J. Volcanol. Geotherm. Res. 300:48–57. http://dx.doi.org/10.1016/j.jvolgeores.2015.01.004.

Carn, S.A., Clarisse, L., Prata, A.J., 2016. Multi-decadal satellite measurements of global volcanic degassing. J. Volcanol. Geotherm. Res. 311:99–134. http://dx.doi.org/10.1016/j.jvolgeores.2016.01.002.

Carn, S.A., Fioletov, V.E., McLinden, C.A., Li, C., Krotkov, N.A., 2017. A decade of global volcanic SO_2 emissions measured from space. Sci Rep 7:44095. http://dx.doi.org/10.1038/srep44095.

Chance, K., Kurucz, R.L., 2010. An improved high-resolution solar reference spectrum for earth's atmosphere measurements in the ultraviolet, visible, and near infrared. J. Quant. Spectrosc. Radiat. Transf. 111, 1289–1295.

Chorowicz, J., Deffontaines, B., Huaman-Rodrigo, D., Guillande, R., Leguern, F., Thouret, J.C., 1992. SPOT satellite monitoring of the eruption of Nevado Sabancaya volcano (Southern Peru). Remote Sens. Environ. 42:43–49. http://dx.doi.org/10.1016/0034-4257(92)90066-S.

Clarisse, L., Coheur, P.-F., Theys, N., Hurtmans, D., Clerbaux, C., 2014. The 2011 Nabro eruption, a SO_2 plume height analysis using IASI measurements. Atmos. Chem. Phys. 14:3095–3111. http://dx.doi.org/10.5194/acp-14-3095-2014.

Coppola, D., Macedo, O., Ramos, D., Finizola, A., Delle Donne, D., del Carpio, J., White, R., McCausland, W., Centeno, R., Rivera, M., Apaza, F., Ccallata, B., Chilo, W., Cigolini, C., Laiolo, M., Lazarte, I., Machaca, R., Masias, P., Ortega, M., Puma, N., Taipe, E., 2015. Magma extrusion during the Ubinas 2013–2014 eruptive crisis based on satellite thermal imaging (MIROVA) and ground-based monitoring. J. Volcanol. Geotherm. Res. 302:199–210. http://dx.doi.org/10.1016/j.jvolgeores.2015.07.005.

Fischer, T.P., 2008. Fluxes of volatiles (H_2O, CO_2, N_2, Cl, F) from arc volcanoes. Geochem. J. 42:21–38. http://dx.doi.org/10.2343/geochemj.42.21.

Gerbe, M.-C., Thouret, J.-C., 2004. Role of magma mixing in the petrogenesis of tephra erupted during the 1990–98 explosive activity of Nevado Sabancaya, southern Peru. Bull. Volcanol. 66:541–561. http://dx.doi.org/10.1007/s00445-004-0340-3.

Giggenbach, W.F., 1987. Redox processes governing the chemistry of fumarolic gas discharges from White Island, New Zealand. Appl. Geochem. 2:143–161. http://dx.doi.org/10.1016/0883-2927(87)90030-8.

Giggenbach, W., 1996. Chemical composition of volcanic gases. In: Scarpa, R., Tilling, R.I. (Eds.), Monit. Mitig. Volcano Hazards, pp. 202–226.

Global Volcanism Program, Smithsonian Institution, 2013. In: Venzke, E. (Ed.), Volcanoes of the World.

Hilton, D.R., Fischer, T.P., Marty, B., 2002. Noble gases and volatile recycling at subduction zones. Rev. Mineral. Geochem. 47:319–370. http://dx.doi.org/10.2138/rmg.2002.47.9.

Instituto Geofísico del Perú (IGP), 2013. Observatorio Vulcanológico del Sur, Reportes Vulcanologicos. Available at: http://ovs.igp.gob.pe/reportes-vulcanologicos.

Instituto Geofísico del Perú (IGP), 2014. Observatorio Vulcanológico del Sur, Reportes Vulcanologicos Available at: http://ovs.igp.gob.pe/reportes-vulcanologicos.

Jay, J.A., Delgado, F.J., Torres, J.L., Pritchard, M.E., Macedo, O., Aguilar, V., 2015. Deformation and seismicity near Sabancaya volcano, southern Peru, from 2002 to 2015. Geophys. Res. Lett. 42. http://dx.doi.org/10.1002/2015GL063589 (2015GL063589).

Kantzas, E.P., McGonigle, A.J.S., Tamburello, G., Aiuppa, A., Bryant, R.G., 2010. Protocols for UV camera volcanic SO_2 measurements. J. Volcanol. Geotherm. Res. 194:55–60. http://dx.doi.org/10.1016/j.jvolgeores.2010.05.003.

Kazahaya, K., Shinohara, H., Saito, G., 1994. Excessive degassing of Izu-Oshima volcano: magma convection in a conduit. Bull. Volcanol. 56:207–216. http://dx.doi.org/10.1007/BF00279605.

Kern, C., Werner, C., Elias, T., Sutton, A.J., Lübcke, P., 2013. Applying UV cameras for SO_2 detection to distant or optically thick volcanic plumes. J. Volcanol. Geotherm. Res. 262:80–89. http://dx.doi.org/10.1016/j.jvolgeores.2013.06.009.

Moussallam, Y., Oppenheimer, C., Aiuppa, A., Giudice, G., Moussallam, M., Kyle, P., 2012. Hydrogen emissions from Erebus volcano, Antarctica. Bull. Volcanol. 74:2109–2120. http://dx.doi.org/10.1007/s00445-012-0649-2.

Moussallam, Y., Peters, N., Ramírez, C., Oppenheimer, C., Aiuppa, A., Giudice, G., 2014. Characterisation of the magmatic signature in gas emissions from Turrialba Volcano, Costa Rica. Solid Earth 5:1341–1350. http://dx.doi.org/10.5194/se-5-1341-2014.

Moussallam, Y., Oppenheimer, C., Scaillet, B., Buisman, I., Kimball, C., Dunbar, N., Burgisser, A., Ian Schipper, C., Andújar, J., Kyle, P., 2015. Megacrystals track magma convection between reservoir and surface. Earth Planet. Sci. Lett. 413:1–12. http://dx.doi.org/10.1016/j.epsl.2014.12.022.

Moussallam, Y., Bani, P., Curtis, A., Barnie, T., Moussallam, M., Peters, N., Schipper, C.I., Aiuppa, A., Giudice, G., Amigo, Á., Velasquez, G., Cardona, C., 2016. Sustaining persistent lava lakes: observations from high-resolution gas measurements at Villarrica volcano, Chile. Earth Planet. Sci. Lett. 454:237–247. http://dx.doi.org/10.1016/j.epsl.2016.09.012.

Moussallam, Y., Peters, N., Masias, P., Apaza, F., Barnie, T., Schipper, C.I., Curtis, A., Tamburello, G., Aiuppa, A., Bani, P., Giudice, G., Pieri, D., Davies, A.G., Oppenheimer, C., 2017. Magmatic gas percolation through the old lava dome of El Misti volcano. Bull. Volcanol. 79:46. http://dx.doi.org/10.1007/s00445-017-1129-5.

Observatorio Vulcanológico del INGEMMET (OVI), 2013. Reportes. Available at: http://ovi.ingemmet.gob.pe/.

Observatorio Vulcanológico del INGEMMET (OVI), 2014. Reportes. Available at: http://ovi.ingemmet.gob.pe/.

Observatorio Vulcanológico del INGEMMET (OVI), 2015. Reportes. Available at: http://ovi.ingemmet.gob.pe/.

Oppenheimer, C., Lomakina, A.S., Kyle, P.R., Kingsbury, N.G., Boichu, M., 2009. Pulsatory magma supply to a phonolite lava lake. Earth Planet. Sci. Lett. 284, 392–398.

Pering, T.D., Tamburello, G., McGonigle, A.J.S., Aiuppa, A., Cannata, A., Giudice, G., Patanè, D., 2014. High time resolution fluctuations in volcanic carbon dioxide degassing from Mount Etna. J. Volcanol. Geotherm. Res. 270:115–121. http://dx.doi.org/10.1016/j.jvolgeores.2013.11.014.

Peters, N., Oppenheimer, C., Killingsworth, D.R., Frechette, J., Kyle, P., 2014. Correlation of cycles in Lava Lake motion and degassing at Erebus Volcano, Antarctica. Geochem. Geophys. Geosyst. 15:3244–3257. http://dx.doi.org/10.1002/2014GC005399.

Platt, U., Stutz, J., 2008. Differential absorption spectroscopy. Differential Optical Absorption Spectroscopy, Physics of Earth and Space Environments. Springer, Berlin Heidelberg:pp. 135–174 http://dx.doi.org/10.1007/978-3-540-75776-4_6.

Pyle, D.M., Mather, T.A., 2009. Halogens in igneous processes and their fluxes to the atmosphere and oceans from volcanic activity: a review. Chem. Geol. 263:110–121. http://dx.doi.org/10.16/j.chemgeo.2008.11.013.

Rivera, M., Thouret, J.-C., Gourgaud, A., 1998. Ubinas, el volcán más activo del sur del Perú desde 1550: Geología y evaluación de las amenazas volcánicas. Bol. Soc. Geol. Perú 88, 53–71.

Rivera, M., Thouret, J.-C., Mariño, J., Berolatti, R., Fuentes, J., 2010. Characteristics and management of the 2006–2008 volcanic crisis at the Ubinas volcano (Peru). J. Volcanol. Geotherm. Res. 198:19–34. http://dx.doi.org/10.1016/j.jvolgeores.2010.07.020.

Rivera, M., Thouret, J.-C., Samaniego, P., Le Pennec, J.-L., 2014. The 2006–2009 activity of the Ubinas volcano (Peru): petrology of the 2006 eruptive products and insights into genesis of andesite magmas, magma recharge and plumbing system. J. Volcanol. Geotherm. Res. 270:122–141. http://dx.doi.org/10.1016/j.jvolgeores.2013.11.010.

Shinohara, H., 2005. A new technique to estimate volcanic gas composition: plume measurements with a portable multi-sensor system. J. Volcanol. Geotherm. Res. 143:319–333. http://dx.doi.org/10.16/j.jvolgeores.2004.12.004.

Shinohara, H., 2008. Excess degassing from volcanoes and its role on eruptive and intrusive activity. Rev. Geophys. 46, RG4005. http://dx.doi.org/10.1029/2007RG000244.

Please cite this article as: Moussallam, Y., et al., Volcanic gas emissions and degassing dynamics at Ubinas and Sabancaya volcanoes; implications for the volatile budget of the centr..., J. Volcanol. Geotherm. Res. (2017), http://dx.doi.org/10.1016/j.jvolgeores.2017.06.027

Shinohara, H., 2013. Volatile flux from subduction zone volcanoes: insights from a detailed evaluation of the fluxes from volcanoes in Japan. J. Volcanol. Geotherm. Res. 268:46–63. http://dx.doi.org/10.1016/j.jvolgeores.2013.10.007.

Shinohara, H., Tanaka, H.K.M., 2012. Conduit magma convection of a rhyolitic magma: constraints from cosmic-ray muon radiography of Iwodake, Satsuma-Iwojima volcano, Japan. Earth Planet. Sci. Lett. 349–350:87–97. http://dx.doi.org/10.1016/j.epsl.2012.07.002.

Stull, D.R., Westrum, E.F., Sinke, G.C., 1969. The Chemical Thermodynamics of Organic Compounds. J. Wiley.

Tamburello, G., 2015. Ratiocalc: software for processing data from multicomponent volcanic gas analyzers. Comput. Geosci. 82:63–67. http://dx.doi.org/10.1016/j.cageo.2015.05.004.

Tamburello, G., Kantzas, E.P., McGonigle, A.J.S., Aiuppa, A., 2011. Vulcamera: a program for measuring volcanic SO_2 using UV cameras. Ann. Geophys. 54. http://dx.doi.org/10.4401/ag-5181.

Tamburello, G., Aiuppa, A., McGonigle, A.J.S., Allard, P., Cannata, A., Giudice, G., Kantzas, E.P., Pering, T.D., 2013. Periodic volcanic degassing behavior: the Mount Etna example. Geophys. Res. Lett. 40:4818–4822. http://dx.doi.org/10.1002/grl.50924.

Tamburello, G., Hansteen, T.H., Bredemeyer, S., Aiuppa, A., Tassi, F., 2014. Gas emissions from five volcanoes in northern Chile and implications for the volatiles budget of the Central Volcanic Zone. Geophys. Res. Lett. 41. http://dx.doi.org/10.1002/2014GL060653 (2014GL060653).

Thouret, J.C., Guillande, R., Huaman, D., Gourgaud, A., Salas, G., Chorowicz, J., 1994. L'Activite actuelle du Nevado Sabancaya (sud Perou); reconnaissance geologique et satellitaire, evaluation et cartographie des menaces volcaniques. Bull. Soc. Geol. Fr. 165, 49–63.

Thouret, J.-C., Rivera, M., Wörner, G., Gerbe, M.-C., Finizola, A., Fornari, M., Gonzales, K., 2005. Ubinas: the evolution of the historically most active volcano in southern Peru. Bull. Volcanol. 67:557–589. http://dx.doi.org/10.1007/s00445-004-0396-0.

Travada, Córdova, V., 1752. El suelo de Arequipa convertido en cielo: historia general de Arequipa, año de 1752 (Arequipa).

Vandaele, A.C., Simon, P.C., Guilmot, J.M., Carleer, M., Colin, R., 1994. SO_2 absorption cross section measurement in the UV using a Fourier transform spectrometer. J. Geophys. Res. Atmos. 99:25599–25605. http://dx.doi.org/10.1029/94JD02187.

Zacámola, Jáuregui, 1784. In: Barriga, V.M. (Ed.), Los Terremotos en Arequipa:1582–1868, La Colmena (1951). (Arequipa).

Please cite this article as: Moussallam, Y., et al., Volcanic gas emissions and degassing dynamics at Ubinas and Sabancaya volcanoes; implications for the volatile budget of the centr..., J. Volcanol. Geotherm. Res. (2017), http://dx.doi.org/10.1016/j.jvolgeores.2017.06.027